Polymer Friction

DOI: 10.1002/anie.201301255

Nanoscale Friction Mechanisms at Solid–Liquid Interfaces**

*Bizan N. Balzer, Markus Gallei, Moritz V. Hauf, Markus Stallhofer, Lorenz Wiegleb, Alexander Holleitner, Matthias Rehahn, and Thorsten Hugel**

Low-friction surfaces and coatings are crucial for miniaturized moving components[1] with a high surface to volume ratio. Therefore, understanding the processes underlying nanoscale friction is essential to design optimized nanoscopic components.[2] Prominent examples of friction effects are the squeaking sound of chalk on a blackboard, the traction of vehicles, or the music from bowed instruments. Such macroscopic observations have led to a couple of phenomenological friction laws, such as Amontons' law, the Rouse model, or Stokes' law.[3] In search for an underlying mechanism for the mainly empirical laws and models to date, many experiments based on the atomic force microscope (AFM)[4] and surface force apparatus (SFA) have been performed.[5] They have led to the view that asperities come constantly in and out of contact[2b,6] or that chemical bonds are broken and reformed in a cooperative manner.[7] This mechanism is usually called stick. Herein we term it cooperative stick to distinguish it from the desorption stick explained below. Both views are accordable with non-uniform friction, leading to a succession of stick and slip events.[5,8]

Our nanoscale measurements with a single polymer as probe reveal the previously experimentally and theoretically described slip (Figure 1 a) and cooperative stick (Figure 1 c).[9] Furthermore, our data necessitates an additional and more frequent mechanism, which we term desorption stick. The model given in Figure 1 b is based on several thousand force–extension traces with various polymer–solvent–substrate combinations as detailed in the following and the Supporting Information (Table S1 and Figures S1–S4). It results from our observation that the friction force is independent of normal force, velocity, and adsorbed polymer length, in contrast to previously described friction mechanisms. As we show that a large variety of these polymers and substrates are dominated by a succession of desorption stick and slip, our results may prove essential to develop novel low-friction surfaces.[10]

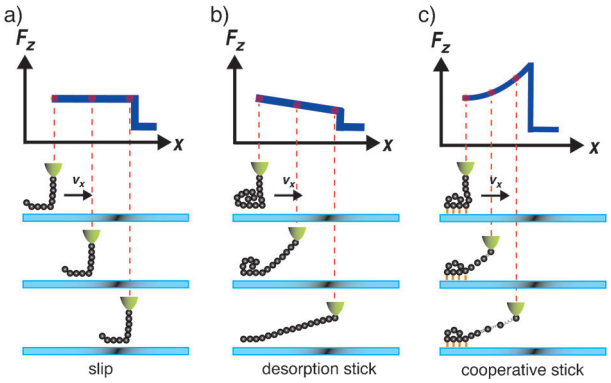

Figure 1. Observed nanoscale friction mechanisms. A single polymer molecule at a solid–liquid interface can respond in different ways to a lateral external force, here exerted by an AFM cantilever tip (depicted in yellow). a) Previously theoretically described slip occurs when the polymer has a very high mobility and undetectably low friction (0.1 pN for our AFM setup). In this case, the vertical force (F_z) versus lateral extension (x) plot shows a plateau of constant force, before the polymer detaches from the surface and F_z becomes zero. b) The most frequent motif is desorption stick. It is characteristically a decrease in the force F_z with increasing lateral pulling extension x. Here the static friction coefficient is high enough to favor desorption over slipping. While the polymer does not move laterally, it leaves the surface continuously with very low internal friction, that is, the polymer is confined in two dimensions. c) In several cases the polymer is stuck to the surface owing to strong directional bonds (indicated as orange sticks); that is, confined in three dimensions (cooperative stick). A lateral external force elastically stretches the polymer. In the images, one sphere corresponds to at least 100 monomers.

We exploit an AFM-based approach that measures both friction[9b] and adhesion forces[11] in one experiment while decoupling them. To that aim, a functionalized AFM cantilever tip is brought in contact with a surface. Then the polymer is pulled up to a certain height by retracting the AFM cantilever tip for more than 100 nm, which is more than an order of magnitude higher than the cantilever deflection (< 10 nm). Then the partly adsorbed single polymer is pulled laterally over the substrate perpendicular to the cantilever axis. Frictional forces are investigated using the vertical cantilever deflection force F_z. The friction force F_R is determined from F_z using the pulling geometry as given in

[*] B. N. Balzer, L. Wiegleb, Prof. Dr. T. Hugel
IMETUM und Physik Department
Technische Universität München
Boltzmannstrasse 11, 85748 Garching (Germany)
E-mail: thugel@mytum.de
Homepage: http://bio.ph.tum.de/home/e22-prof-dr-hugel/
Dr. M. Gallei, Prof. Dr. M. Rehahn
Ernst-Berl Institut für Makromolekulare Chemie
Technische Universität Darmstadt
Petersenstrasse 22, 64287 Darmstadt (Germany)
M. V. Hauf, M. Stallhofer, Prof. Dr. A. Holleitner
Walter Schottky Institut and Physik Department
Technische Universität München
Am Coulombwall 4a, 85748 Garching (Germany)

[**] Helpful discussions with Robijn Bruinsma, Roland Netz, Matthias Rief, Hermann Gaub, Nolan Holland, Dominik Horinek, Jose Garrido, Aykut Erbas, Matthias Erdmann, Sandra Kienle, Stefanie Krysiak, Bettina Kracke, Tobias Pirzer, and Frank Stetter are gratefully acknowledged. We thank the Deutsche Forschungsgemeinschaft (Hu 997/2-2, Re-923/14-2), priority program SPP1369 and Nanosystems Initiative Munich (NIM) for financial support.

Supporting information for this article is available on the WWW under http://dx.doi.org/10.1002/anie.201301255.

Figure 2a. At any time the positive force axis represents adhesive interactions.

This combination of desorption in the z direction and lateral pulling finally results in a detection limit of less than 1 pN for the friction force of a single polymer. The adsorbed

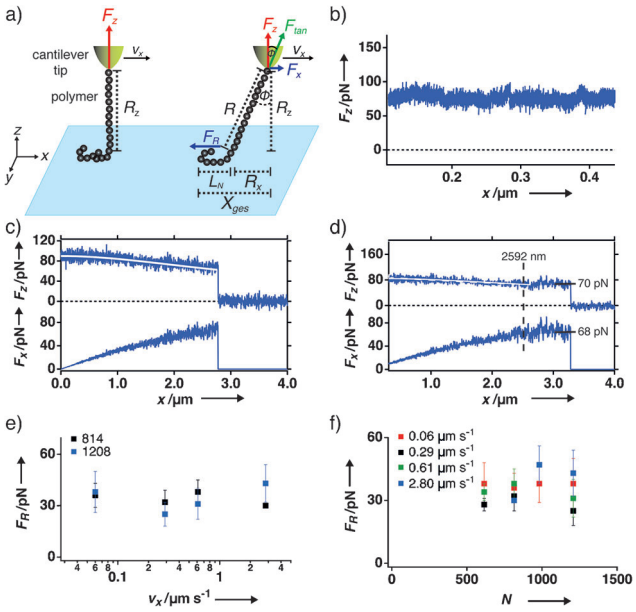

Figure 2. Nanoscale friction: slip and desorption stick. a) The AFM experiment to detect single polymer friction by lateral pulling. The friction force F_R is geometrically defined by the measured F_z, R_x, and R_z. R_z is the fixed z extension between AFM cantilever tip and substrate, F_z the vertical force component, F_{tan} the force acting along the polymer, F_x the lateral force component, ϕ the polymer angle between a tangent to the polymer and the normal to the substrate, L_N the adsorbed polymer length, and v_x the lateral pulling velocity. b) Typical F_z versus lateral extension (x) trace for PGA on PTFE in H_2O showing a constant F_z value resembling slip. c) Typical F_z and F_x versus x curve for PS on PTFE in H_2O. Here, F_x is smaller than F_R until the polymer desorbs at around 2.8 µm. d) Typical F_z and F_x versus x trace for PS on PTFE in H_2O with a desorption stick event followed by slip where F_x balances F_R at around 2.6 µm (indicated by a dashed black line). The white lines show F_z from Equation (1). e) Dependence of friction force F_R on pulling velocity v_x for the adsorbed monomer number of N: 814 (black) and 1206 (blue) for PSPI on H-terminated diamond in H_2O. f) F_R dependence on adsorbed monomer number N for the velocities v_x: 0.06 µm s^{-1} (red), 0.29 µm s^{-1} (black), 0.61 µm s^{-1} (green), and 2.80 µm s^{-1} (blue) for PSPI on H-terminated diamond in H_2O.

polymer length can be determined with nanometer precision (see the Supporting Information). Our approach has several advantages over experiments measuring the free diffusion of a (labeled) polymer[12] and utilizing the Einstein relation to determine the friction coefficient. In particular, we are able to obtain the dependence on the controlled pulling velocity, adhesion force, and adsorbed polymer length for every single polymer. These are essential to develop a molecular picture of single polymer friction.

Figure 2b shows the vertical force F_z versus the laterally moved extension x for a typical lateral pulling experiment of poly(glutamic acid) (PGA) on poly(tetrafluorethylene) (PTFE) in H_2O. The constant plateau force shows that the polymer is highly mobile in the plane of the substrate, resembling a slip event ($F_x = F_R$ below 0.1 pN). By contrast, Figure 2c shows the lateral pulling for a single polystyrene (PS) on PTFE in H_2O. The resulting event causes a decrease in F_z from 90 pN to a value of 71 pN at 2.8 µm. Based on previous theoretical treatment,[9] the angular dependence of F_z is given by Equation (1):

$$F_z = F_{tan} \cdot \cos\left(\arctan(R_x \cdot R_z^{-1})\right) \quad (1)$$

where F_{tan} is the force component acting along the polymer backbone and keeping the polymer stretched during lateral pulling. At the same time, the lateral force F_x increases to about 77 pN (bottom of Figure 2c), before the polymer detaches from the substrate and both F_z and F_x drop to zero. This cannot be explained by slip or cooperative stick and is first evidence for the model depicted in Figure 1b. The increase of lateral force F_x can be explained by a part of the polymer sticking at a constant position with respect to the substrate, while the main body of the polymer continuously desorbs into solution until it detaches from the substrate (Figure 1b). Here the static friction coefficient is high enough to favor desorption over slipping. F_z from Equation (1) (white lines in Figure 2c,d) matches our data very well.

Figure 2d shows a desorption stick followed by a slip event for PS on PTFE in H_2O, which allows the friction force F_R to be determined for this desorption stick mechanism. While F_z decreases, the polymer angle ϕ increases until the force component F_x counterbalances F_R at about 2.6 µm and the polymer starts to slip. F_R is then given by Equation (2):

$$F_R = F_x = R_x \cdot R_z^{-1} \cdot F_z \quad (2)$$

where the polymer angle ϕ is given by $\tan\phi = R_x \cdot R_z^{-1}$. In the depicted example, $F_z = 70$ pN, which results in $F_R = 68$ pN and $\phi = 44°$ (see the Supporting Information, Table S2, for more examples).

In the following, we discuss how the friction force of the desorption stick behavior depends on velocity and polymer length. Figure 2e and Figure 2f show the friction force F_R versus velocity v_x and adsorbed polymer length L_N represented by the monomer number N, for a PS-based polymer (called PSPI; Supporting Information, Figure S5) on H-terminated diamond in H_2O. Surprisingly, the friction force does not significantly depend on the velocity or on the adsorbed polymer length. This already renders the Rouse model, as used to determine the viscous frictional force of single polymers on solid substrates, inappropriate for desorption stick. This kind of model is given by $F_R = \mu \cdot v$ with μ being the polymer friction coefficient and v the polymer sliding velocity. μ can have Rouse ($\mu \sim N$),[9b,13] sub-linear ($\mu \sim N^{3/4}$),[14] or super-linear scaling ($\mu \sim N^{3/2}$).[13c,15] The independence of friction force on pulling velocity in the examined range places our measurements in the boundary friction regime.[3]

To further characterize this friction mechanism, we probed the role of surface topography. We investigated PSPI on structured gallium arsenide (GaAs) in H_2O. The GaAs surface has lateral structures with a periodicity of

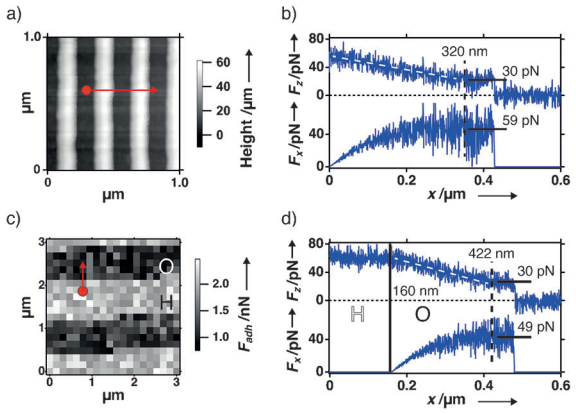

Figure 3. Effect of surface topography and chemistry on nanoscale friction. a) AFM image of patterned GaAs to investigate the effect of surface topography. Lateral pulling is performed along the red line with arrow. b) Typical vertical (F_z) and lateral (F_x) force versus lateral extension (x) curve of a PS-based polymer across topographically patterned GaAs in H_2O (dashed white lines indicate the desorption stick event). As expected for desorption stick, the traces next to the pattern show the same behavior. c) Force map of an O/H-terminated diamond surface. The H-terminated region shows higher AFM cantilever tip–substrate interaction F_{adh} than the O-terminated region. The force maps enable us to define pulling paths across the O/H-boundary (red line with arrow). d) Typical F_z versus x and F_x versus x trace for PGA on diamond in H_2O (dashed white lines indicate desorption stick event). The crossing of the O/H-boundary is indicated in the lateral pulling trace by a vertical black line. Dashed black lines indicate the transition from desorption stick to slip.

120 nm to 150 nm and with a depth of about 50 nm (Figure 3a; Supporting Information, Figure S6). The friction curves do not show any difference between the structured and the unstructured GaAs areas (a typical trace is shown in Figure 3b). In particular, the slope in the F_z versus x graph as well as the height of the final force plateau before detachment are similar (around 30 pN; Supporting Information, Figure S2). Furthermore, further studies reveal that the friction force and mechanism on PTFE, oxygen-, and hydrogen-terminated diamond, hydrophobic self-assembled monolayers of alkanthiols on Au (SAMs) and mica is not related to their roughness (Supporting Information, Table S1 and Figure S8). In summary, we find that the friction behavior marginally depends on surface topography or on surface defects. We believe that the polymer does not span over or undergo interlock with surface asperities, unlike the prevailing view for macroscopic bodies.[2b]

Next we probed the effect of chemical surface termination in a controlled manner: we patterned monocrystalline diamond with oxygen and hydrogen termination by electron-beam lithography and exposure to oxygen or hydrogen plasma. The pattern is confirmed by friction force microscopy (Supporting Information, Figure S7). The O/H pattern enables us to compare friction on hydrophilic and hydrophobic substrate in a single measurement. To position the polymer at a defined spot, we performed a force map prior to every single polymer friction experiment. Figure 3c shows such a force map and indicates the lateral pulling paths of the polymer across the surface for the data depicted in Figure 3d. Here the friction curve starts in an H-terminated area and crosses the O/H-boundary. In the H-terminated section, PGA results in a constant plateau force F_z during lateral pulling; that is, slip behavior with undetectably low friction force. As soon as O-termination is reached, the polymer exhibits desorption stick. As the adhesion force on these two surface terminations differs less than 10 pN (Supporting Information, Table S2 and Figure S9), we conclude that desorption stick behavior is largely independent of adhesion force.

For polymer systems, the following version of Amontons' law is suggested for strongly adsorbing bodies with friction coefficient μ and the normal force being divided into load F_L and adhesion force F_{adh}: $F_R = \mu\cdot(F_L + F_{adh})$.[3b] In case of single polymers, the load is negligible, leading to a linear dependence of F_R on F_{adh}, which is represented by the desorption force F_{des} (Supporting Information, Figure S9). Such a linear dependence is incompatible with desorption stick. Instead, we explain the behavior by a dominating effect of the polymer conformation induced by the solvent as discussed in the following.

In general, direct solvent-related polymer friction is below our detection limit and thus contributes by less than 0.1 pN to the total measured friction force. As we pull PSPI across the substrates discussed above in the bad solvent H_2O, we observe desorption stick for most traces: F_z decreases linearly until slip or detachment of the polymer from the substrate occurs. Measurements in chloroform (Supporting Information, Figure S1), which is a better solvent for PS based polymers than H_2O,[3b,13a] show friction below our detection limit. Thus, the friction forces are at least two orders of magnitude lower than in H_2O, although the viscosity is only reduced by half.[16]

We interpret these findings such that the solvent causes a desorption stick behavior by a lateral confinement of the polymer on the substrate. To move the polymer across the surface, a significant amount of solvent has to be displaced simultaneously, resulting in forces of several tens of pN (Supporting Information, Table S2). In this case, desorption is favored compared to lateral movement for large parts of the friction experiment. For example, we detect desorption stick in more than 80% of the traces on an O-terminated diamond. This interpretation is consistent with what we observe for PGA on PTFE in H_2O, which is a good solvent in this system (Figure 2b).

We point out that our technique is sensitive enough to directly detect the well-known stick–slip effect at the nanoscale.[5,8] Figure 4 shows a respective trace for PGA on

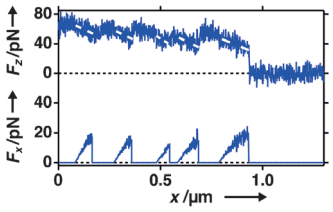

Figure 4. Nanoscale stick–slip. Vertical (F_z) and lateral force (F_x) versus lateral extension (x) for PGA on a hydrophobic SAM in H_2O. Repeated succession between slip and desorption stick events is observed. The latter are indicated by the dashed white lines.

a hydrophobic SAM in H_2O. We can exclude that the periodicity of stick–slip directly reflects the surface pattern: we observe different stick–slip patterns for consecutive traces with one and the same polymer on the same surface along the same line (Supporting Information, Figure S4).

We note that apart from slip and desorption stick, we occasionally observe cooperative stick. There, the polymer is stretched up to a point where the bonds between substrate and polymer break and the polymer detaches (Supporting Information, Figure S3). Such traces have been found for vertical pulling before, but not for lateral pulling.[17] They require the absence of fast internal relaxation of the polymer. The part of the polymer in between the AFM cantilever tip and the substrate is elastically stretched, resembling the well-known wormlike chain increase in force.[19] This appears never on H-terminated diamond and only in about 10% of the traces on O-terminated diamond. It is always present on hydrophilic surfaces, as shown by poly(allylamine) on mica (Supporting Information, Figure S3). We speculate that in this case strong directional bonds, in particular hydrogen bonds, prevent internal relaxation.[7,13b]

We point out the following four essential insights to describe our results. First, good solvent and a homogenously hydrophobic substrate result in slip without stick events. Second, bad solvents cause desorption stick irrespective of the substrate. Third, the strong formation of directional bonds (for example, hydrogen bonds) results in stretching of the polymer (cooperative stick). Fourth, all intermediate cases lead to a significant and dominating amount of desorption stick.

In conclusion, our AFM-based method allowed us to find and characterize a friction mechanism that is independent of normal force, polymer length, and velocity. This contrasts friction models based on Amontons' law and the Rouse model. We term this mechanism desorption stick. Here, vertical and lateral pulling have basically the same effect, rendering the mechanism independent of the polymer angle ϕ. Therefore, this process is mechanistically and conceptually very distinct from DNA shearing and unzipping.[18] As many frictional processes are dominated by the periods of stick in between slip events, we anticipate that our characterization of desorption stick will guide the bottom-up development of durable, low-friction surface coatings in polymer-based nanotechnology.

Received: February 12, 2013
Revised: March 27, 2013
Published online: May 10, 2013

Keywords: adsorption · nanotribology · polymers · single-molecule force spectroscopy · surface patterning

[1] M. A. Lantz, D. Wiesmann, B. Gotsmann, *Nat. Nanotechnol.* **2009**, *4*, 586 – 591.
[2] a) R. W. Carpick, *Science* **2006**, *313*, 184 – 185; b) M. Urbakh, J. Klafter, D. Gourdon, J. Israelachvili, *Nature* **2004**, *430*, 525 – 528; c) Z. L. Wang, W. Wu, *Angew. Chem.* **2012**, *124*, 11868 – 11891; *Angew. Chem. Int. Ed.* **2012**, *51*, 11700 – 11721.
[3] a) B. Bhushan, *Introduction to Tribology*, Wiley, New York, **2002**; b) H. Butt, M. Kappl, *Surface and Interfacial Forces*, *1st ed.*, Wiley-VCH, Weinheim, **2010**.
[4] a) C. M. Mate, G. M. McClelland, R. Erlandsson, S. Chiang, *Phys. Rev. Lett.* **1987**, *59*, 1942 – 1945; b) R. W. Carpick, M. Salmeron, *Chem. Rev.* **1997**, *97*, 1163 – 1194.
[5] H. Yoshizawa, Y. L. Chen, J. Israelachvili, *J. Phys. Chem.* **1993**, *97*, 4128 – 4140.
[6] a) A. Socoliuc, E. Gnecco, S. Maier, O. Pfeiffer, A. Baratoff, R. Bennewitz, E. Meyer, *Science* **2006**, *313*, 207 – 210; b) R. J. Cannara, M. J. Brukman, K. Cimatu, A. V. Sumant, S. Baldelli, R. W. Carpick, *Science* **2007**, *318*, 780 – 783.
[7] A. Erbas, D. Horinek, R. R. Netz, *J. Am. Chem. Soc.* **2012**, *134*, 623 – 630.
[8] a) W. F. Brace, J. D. Byerlee, *Science* **1966**, *153*, 990 – 992; b) P. A. Thompson, M. O. Robbins, *Science* **1990**, *250*, 792 – 794.
[9] a) A. Serr, R. R. Netz, *Europhys. Lett.* **2006**, *73*, 292 – 298; b) F. Kühner, M. Erdmann, L. Sonnenberg, A. Serr, J. Morfill, H. E. Gaub, *Langmuir* **2006**, *22*, 11180 – 11186.
[10] H. Bhaskaran, B. Gotsmann, A. Sebastian, U. Drechsler, M. A. Lantz, M. Despont, P. Jaroenapibal, R. W. Carpick, Y. Chen, K. Sridharan, *Nat. Nanotechnol.* **2010**, *5*, 181 – 185.
[11] T. Hugel, M. Seitz, *Macromol. Rapid Commun.* **2001**, *22*, 989 – 1016.
[12] B. Maier, J. O. Radler, *Phys. Rev. Lett.* **1999**, *82*, 1911 – 1914.
[13] a) M. Rubinstein, R. H. Colby, *Polymer Physics*, Oxford University Press, New York, **2003**; b) A. Serr, D. Horinek, R. R. Netz, *J. Am. Chem. Soc.* **2008**, *130*, 12408 – 12413; c) D. Mukherji, G. Bartels, M. H. Mueser, *Phys. Rev. Lett.* **2008**, *100*, 068301.
[14] T. G. Desai, P. Keblinski, S. K. Kumar, S. Granick, *Phys. Rev. Lett.* **2007**, *98*, 218301.
[15] S. A. Sukhishvili, Y. Chen, J. D. Muller, E. Gratton, K. S. Schweizer, S. Granick, *Nature* **2000**, *406*, 146 – 146.
[16] J. A. Dean, *Lange's Handbook of Chemistry*, *15th ed.*, McGraw-Hill, New York, **1999**.
[17] a) H. J. Butt, B. Cappella, M. Kappl, *Surf. Sci. Rep.* **2005**, *59*, 1 – 152; b) M. S. Z. Kellermayer, S. B. Smith, H. L. Granzier, C. Bustamante, *Science* **1997**, *276*, 1112 – 1116; c) M. Rief, F. Oesterhelt, B. Heymann, H. E. Gaub, *Science* **1997**, *275*, 1295 – 1297; d) S. B. Smith, Y. J. Cui, C. Bustamante, *Science* **1996**, *271*, 795 – 799; e) B. N. Balzer, T. Hugel, *Polymer Science*: *A Comprehensive Reference*, *Vol. 2* (Eds.: K. Matyjaszewski, M. Möller), Elsevier, Amsterdam, **2012**, pp. 629 – 645.
[18] a) T. Strunz, K. Oroszlan, R. Schafer, H. J. Guntherodt, *Proc. Natl. Acad. Sci. USA* **1999**, *96*, 11277 – 11282; b) S. K. Kufer, M. Strackharn, S. W. Stahl, H. Gumpp, E. M. Puchner, H. E. Gaub, *Nat. Nanotechnol.* **2009**, *4*, 45 – 49.
[19] J. F. Marko, E. D. Siggia, *Macromolecules* **1995**, *28*, 8759 – 8770.

